PHYSICAL REVIEW D **79,** 124014 (2009)

Homoclinic orbits around spinning black holes. II. The phase space portrait

Gabe Perez-Giz[1,*] and Janna Levin[2,3,†]

[1]*Physics Department, Columbia University, New York, New York 10027, USA*
[2]*Department of Physics and Astronomy, Barnard College of Columbia University, 3009 Broadway, New York, New York 10027, USA*
[3]*Institute for Strings, Cosmology and Astroparticle Physics, Columbia University, New York, New York 10027, USA*

(Received 2 December 2008; published 11 June 2009)

In paper I in this series, we found exact expressions for the equatorial homoclinic orbits: the separatrix between bound and plunging, whirling and not whirling motion. As a companion to that physical space study, in this paper we paint a phase space portrait of the homoclinic orbits that includes exact expressions for the actions and fundamental frequencies. Additionally, we develop a reduced Hamiltonian description of Kerr motion that allows us to track groups of trajectories with a single global clock. This facilitates a variational analysis, whose stability exponents and eigenvectors could potentially be useful for future studies of families of black hole orbits and their associated gravitational waveforms.

DOI: 10.1103/PhysRevD.79.124014 PACS numbers: 04.70.−s, 95.30.Sf, 04.25.−g, 04.20.Jb

I. INTRODUCTION

The transition from inspiral to plunge is a crucial landmark in the radiative evolution of a compact object falling into a supermassive black hole. A natural physical divide, the transition is also a natural conceptual divide. While understanding the final orbital cycles might require better knowledge of the gravitational self-force [1] or advances in numerical relativity [2–11], the inspiral can be modeled as adiabatic evolution through a sequence of Kerr geodesics [12–17]. Inspiral gives way to plunge through an important family of separatrices. In paper I in this series [18], we detailed the nature of the separatrix between bound and plunging orbits as a homoclinic orbit—an orbit in the black hole spacetime that whirls an infinite number of times as it asymptotes to an unstable circle. We found exact solutions for the family of homoclinic trajectories and depicted them as the infinite limit of a sequence of zoom-whirls [18]. As a companion to that physical space picture, we analyze the complementary phase space picture here.

Formally, the homoclinic orbit lies on the intersection of the stable and unstable manifolds of a hyperbolic invariant set. A collection of points in phase space is an invariant set if orbits that are in the set at any time remain in the set for all earlier and future times. An invariant set S is hyperbolic if it has both a stable manifold (orbits that approach S as $t \to +\infty$) and an unstable manifold (orbits that approach S as $t \to -\infty$). In the black hole spacetime, the hyperbolic invariant sets are recognized by the more familiar tag "unstable circular orbits." To make this connection precise from the phase space perspective, we examine the variational equations—the equations governing the evolution of small displacements from the circular orbits. It is straightforward to show that the energetically bound, unstable circular orbits are hyperoblic; that is, they have an unstable eigendirection and a stable eigendirection. We then show that the stable and unstable eigendirections are tangent to the homoclinic orbit in the local neighborhood of the unstable circular orbit. In other words, two of the eigensolutions of the variational equations around bound unstable circular orbits are local representations of the homoclinic orbit. These eigensolutions capture the qualitative and quantitative features of the separatrix, including the azimuthal motion [18].

We begin by devising a reduced Hamiltonian formulation of equatorial Kerr motion that naturally admits comparisons of groups of trajectories against a single global clock. The variation of Hamilton's equations yields stability exponents for circular orbits that could have general utility, for instance, as an estimate of inspiral or merger time scales [19,20], or in a coarse graining of the template space around periodic orbits [21]. For completeness, we also find explicit expressions for the actions and the frequencies.

II. KERR HOMOCLINIC ORBITS IN PHASE SPACE

Carter famously reduced the full geodesic equations of motion to four first-order equations in space and time coordinates [22]. Despite the appeal of this accomplishment, a phase space analysis requires variation of the full equations of motion for both the coordinates and their conjugate momenta. For this reason, we will not work in the first-order integrated system of equations, although our analysis will incorporate some features of those familiar expressions. Instead, we write down a Hamiltonian formulation of Kerr geodesic motion and explicitly derive the equations of motion.

A. Kerr equations of motion

Although written out in many places, to remain self-contained we include the Kerr metric in Boyer-Lindquist coordinates and geometrized units ($G = c = 1$):

*gabe@phys.columbia.edu
†janna@astro.columbia.edu

$$ds^2 = -\left(1 - \frac{2Mr}{\Sigma}\right)dt^2 - \frac{4Mar\sin^2\theta}{\Sigma}dtd\varphi + \sin^2\theta\left(r^2 + a^2 + \frac{2Ma^2r\sin^2\theta}{\Sigma}\right)d\varphi^2 + \frac{\Sigma}{\Delta}dr^2 + \Sigma d\theta^2, \quad (1)$$

where M, a denote the central black hole mass and spin angular momentum per unit mass, respectively, and

$$\Sigma \equiv r^2 + a^2\cos^2\theta \qquad \Delta \equiv r^2 - 2Mr + a^2. \quad (2)$$

The constants of motion along Kerr geodesics are the rest mass of the test object, energy E, axial angular momentum L_z, and the Carter constant Q [22].

In dimensionless units, the first-order geodesic equations are [22]

$$\Sigma\dot{r} = \pm\sqrt{R} \quad (3a)$$

$$\Sigma\dot{\theta} = \pm\sqrt{\Theta} \quad (3b)$$

$$\Sigma\dot{\varphi} = \frac{a}{\Delta}(2rE - aL_z) + \frac{L_z}{\sin^2\theta} \quad (3c)$$

$$\Sigma\dot{t} = \frac{(r^2 + a^2)^2E - 2arL_z}{\Delta} - a^2E\sin^2\theta, \quad (3d)$$

where an overdot denotes differentiation with respect to the particle's (dimensionless) proper time τ and

$$\Theta(\theta) = Q - \cos^2\theta\left\{a^2(1 - E^2) + \frac{L_z^2}{\sin^2\theta}\right\} \quad (4)$$

$$R(r) = -(1 - E^2)r^4 + 2r^3 - [a^2(1 - E^2) + L_z^2]r^2 + 2(aE - L_z)^2r - Q\Delta. \quad (5)$$

The four Eqs. (3), though no doubt valuable in many contexts, do not lend themselves to a variational analysis. The formalism we will employ is Hamiltonian and a phase space study requires not just the coordinates but also their conjugate momenta. Although we start from scratch with a Hamiltonian formulation of the dynamical equations, we will make use of the Eqs. (3)–(5) along the way.

We will restrict attention to equatorial orbits and defer nonequatorial motion to a future work. Equatorial Kerr orbits have $\theta = \pi/2$, $\dot{\theta} = 0$, and $Q = 0$.

B. Hamiltonian formulation

The Hamiltonian for a relativistic nonspinning free particle of mass μ is [23]

$$H = \tfrac{1}{2}g^{\alpha\beta}p_\alpha p_\beta, \quad (6)$$

where the inverse metric components $g^{\alpha\beta}$ are functions of the spacetime coordinates and each p_α is both a component of the 4-momentum one-form and the canonical momentum conjugate to coordinate q^α.

We want to build the Hamiltonian explicitly from Eq. (1), and we could do so just by inserting the inverse metric and turning the crank. However, we can yield an equivalent but algebraically nicer expression for the Hamiltonian with far less effort. To begin, consider the terms in the Hamiltonian explicitly containing p_r or p_θ:

$$\tfrac{1}{2}(g^{rr}p_r^2 + g^{\theta\theta}p_\theta^2). \quad (7)$$

Since the r, θ portion of the metric $g_{\mu\nu}$ is diagonal, that block of the inverse metric is also diagonal, with $g^{rr} = 1/g_{rr}$ and $g^{\theta\theta} = 1/g_{\theta\theta}$. The p_r, p_θ terms in H are thus

$$\frac{1}{2}\left(\frac{\Delta}{\Sigma}\right)p_r^2 + \frac{1}{2}\left(\frac{1}{\Sigma}\right)p_\theta^2 \quad (8)$$

The remaining terms in the Hamiltonian will be quadratic in the remaining momenta p_t and p_φ with coefficients that are functions only of r and θ (since the metric, and thus the inverse metric, are cyclic in the t and φ coordinates). The Hamiltonian can therefore be written as

$$H(\mathbf{q}, \mathbf{p}) = \frac{1}{2}\left(\frac{\Delta}{\Sigma}\right)p_r^2 + \frac{1}{2}\left(\frac{1}{\Sigma}\right)p_\theta^2 + \frac{1}{2}F(r, \theta, p_t, p_\varphi), \quad (9)$$

where $F(r, \theta, p_t, p_\varphi) = F(r, \theta, -E, L)$ is some expression equivalent to $g^{tt}p_t^2 + 2g^{t\varphi}p_tp_\varphi + g^{\varphi\varphi}p_\varphi^2$.

Notice that the $\dot{r}$ and $\dot{\theta}$ equations of (3) can be recast as

$$\frac{\Delta}{2\Sigma}p_r^2 - \frac{R}{2\Delta\Sigma} = 0 \qquad \frac{1}{2\Sigma}p_\theta^2 - \frac{\Theta}{2\Sigma} = 0. \quad (10)$$

Adding these equations and subtracting $1/2$ from both sides tells us that

$$\frac{\Delta}{2\Sigma}p_r^2 + \frac{1}{2\Sigma}p_\theta^2 - \frac{R}{2\Delta\Sigma} - \frac{\Theta}{2\Sigma} - \frac{1}{2} = -\frac{1}{2}. \quad (11)$$

Since $H \equiv -1/2$, the left hand side must be identical to H. Matching to Eq. (9), we glean that

$$F(r, \theta, -E, L) = -\frac{R + \Delta\Theta}{\Delta\Sigma} - 1, \quad (12)$$

so that we finally get

$$H = \frac{\Delta}{2\Sigma}p_r^2 + \frac{1}{2\Sigma}p_\theta^2 - \frac{R + \Delta\Theta}{2\Delta\Sigma} - \frac{1}{2}, \quad (13)$$

where R and Θ are the functions in (5). Note that in dimensionless coordinates, the Hamiltonian has the same constant value $-1/2$ along any trajectory. We also used this form of the Hamiltonian in Appendix A of Ref. [21].

Because all dependences on $E \equiv -p_t$ and $L_z \equiv p_\varphi$ are locked inside R and Θ and H is cyclic in t and φ, Hamilton's equations

$$\dot{q}^\mu = \frac{\partial H}{\partial p_\mu}, \qquad \dot{p}_\mu = -\frac{\partial H}{\partial q^\mu} \quad (14)$$

applied to the Hamiltonian (13) yield equations of motion

$$\dot{r} = \frac{\Delta}{\Sigma} p_r,$$

$$\dot{p}_r = -\left(\frac{\Delta}{2\Sigma}\right)' p_r^2 - \left(\frac{1}{2\Sigma}\right)' p_\theta^2 + \left(\frac{R + \Delta\Theta}{2\Delta\Sigma}\right)' \tag{15a}$$

$$\dot{\theta} = \frac{1}{\Sigma} p_\theta,$$

$$\dot{p}_\theta = -\left(\frac{\Delta}{2\Sigma}\right)^\theta p_r^2 - \left(\frac{1}{2\Sigma}\right)^\theta p_\theta^2 + \left(\frac{R + \Delta\Theta}{2\Delta\Sigma}\right)^\theta \tag{15b}$$

$$\dot{\varphi} = -\frac{1}{2\Delta\Sigma}\frac{\partial}{\partial L}(R + \Delta\Theta), \qquad \dot{p}_\varphi = 0 \tag{15c}$$

$$\dot{t} = \frac{1}{2\Delta\Sigma}\frac{\partial}{\partial E}(R + \Delta\Theta), \qquad \dot{p}_t = 0 \tag{15d}$$

where the superscripts $'$ and θ denote differentiation with respect to r and θ, respectively. Notice, all of the Eqs. (15) are dynamically equivalent to Eqs. (3). These equations define an 8D phase space, one axis for each of the 4 coordinates t, r, θ, φ and their corresponding conjugate momenta, with τ parametrizing trajectories in the space. The Hamiltonian (13) derived above governs the evolution of the system in this 8-dimensional phase space.

A manifestly covariant form of Hamilton's equations, equivalent to (14), has been used in other references to deduce important information about *individual* trajectories [22–24]. We, however, want to describe how *multiple* trajectories evolve relative to one another to locate stable and unstable flows in phase space, and that task requires tracking evolution with respect to some global clock. In the covariant Hamiltonian picture, the time parameter τ in (14) flows differently on different trajectories and is thus not a physically viable global clock.[1]

Coordinate time t would be a good global clock, but it becomes awkward to maintain the clock as a coordinate in the 8D phase space. Furthermore, all orbits move monotonically away from the origin along the t direction.[2] Consequently, no region of finite phase volume contains any orbit in its entirety, and there are no recurrent invariant sets.[3]

The 8D space, then, is not a natural backdrop for the discussion of homoclinic orbits. Luckily, it is also not required: by performing a phase space reduction,[4] we can *completely* analyze Kerr motion within a 6D space—the phase space of spatial coordinates and their conjugate momenta parameterized by coordinate time t—that avoids the shortcomings mentioned in the previous two paragraphs with no loss of dynamical information. To understand how 8D information can be captured fully in a 6D framework, we note that the dynamics described by Eqs. (15) is not truly 8D: since $H \equiv -1/2$ on all trajectories, the dynamics is already constrained to a 7D hypersurface in the original 8D phase space. In the covariant formulation, proper time is merely an evolution parameter, and only 7 of the 8 coordinates and momenta are truly independent.

An alternative but physically equivalent formulation considers a phase space spanned by the six spatial coordinates and momenta on which coordinate time t is the evolution parameter and on which an extra function $\tau(\vec{q}, \vec{p})$ (the seventh degree of freedom) is defined for each trajectory. The energy $E = -p_t$ in such a formulation becomes the new Hamiltonian function for the 6D space, just as in classical mechanics:

$$\frac{dq^i}{dt} = \frac{\partial E}{\partial p_i}, \qquad \frac{dp_i}{dt} = -\frac{\partial E}{\partial q^i}. \tag{16}$$

In other words, we can map the relativistic free particle motion to an equivalent classical problem in which t is the evolution parameter, the energy function $E(\vec{q}, \vec{p})$ is the Hamiltonian, and τ appears as an additional dynamical function (which we will never need in this paper and thus do not track). Such a space/time splitting, which amounts simply to a more convenient choice of evolution parameter, is dynamically exact and involves no approximation. All relativistic dynamical effects (like zoom-whirl behavior) are still present. The payoff is that the 6D formalism greatly facilitates our task: there are now bound orbits and recurrent invariant sets, and the evolution parameter for our system (now t instead of τ) is a physically good global clock.

To get the 6D equations of motion for the Kerr system, we could calculate $E(\vec{q}, \vec{p})$ explicitly[5] from

$$H(\vec{q}, \vec{p}, E(\vec{q}, \vec{p})) = -\tfrac{1}{2} \tag{17}$$

and then apply (16). Alternately, we can realize that we have to get the same result if we divide all the spatial equations in (15) by $\dot{t}$ (15d) and immediately write down

[1] Mathematically, of course, τ is a perfectly fine global clock. After all, the Hamiltonian formalism knows nothing about relativity and is perfectly happy to answer physically unsensible questions like how equal τ separations evolve with respect to "global proper time."

[2] Strictly speaking, the motion is also monotonic in the φ direction, but topologically identifying $\varphi = 0$ and $\varphi = 2\pi$ compactifies phase space in the φ direction and thus bounds the φ motion [23].

[3] Of course, every individual trajectory is still a trivial sort of invariant set. Since even in this space, the phase trajectories of homoclinic orbits asymptote at $\tau \to \pm\infty$ to those representing unstable circular orbits, we can still talk about their being homoclinic to an invariant set. Still, the language is inelegant, and having to track the additional t evolution is an unwelcome complication.

[4] Phase space reduction is detailed in numerous dynamical systems texts (e.g. Ref. [25]) and can be applied to any dynamical system, relativistic or otherwise. We also discuss the reduced phase space for Kerr motion briefly in the appendix of [21] and elaborate on its details in a future work.

[5] Since we consider only positive energies, we keep the larger root in the resulting quadratic equation for E.

$$\frac{dr}{dt} = \frac{1}{\dot{t}} \times \frac{\Delta}{\Sigma} p_r,$$
$$\frac{dp_r}{dt} = \frac{1}{\dot{t}} \times \left\{ -\left(\frac{\Delta}{2\Sigma}\right)' p_r^2 - \left(\frac{1}{2\Sigma}\right)' p_\theta^2 + \left(\frac{R + \Delta\Theta}{2\Delta\Sigma}\right)' \right\} \quad (18a)$$
$$\frac{d\theta}{dt} = \frac{1}{\dot{t}} \times \frac{1}{\Sigma} p_\theta,$$
$$\frac{dp_\theta}{dt} = \frac{1}{\dot{t}} \times \left\{ -\left(\frac{\Delta}{2\Sigma}\right)^\theta p_r^2 - \left(\frac{1}{2\Sigma}\right)^\theta p_\theta^2 + \left(\frac{R + \Delta\Theta}{2\Delta\Sigma}\right)^\theta \right\} \quad (18b)$$
$$\frac{d\varphi}{dt} = \frac{1}{\dot{t}} \times \left\{ -\frac{1}{2\Delta\Sigma} \frac{\partial}{\partial L}(R + \Delta\Theta) \right\}, \qquad \frac{dp_\varphi}{dt} = 0 \quad (18c)$$

with the caveat that, when we calculate derivatives of Eqs. (18), every instance of E be treated as a function $E(\vec{q}, \vec{p})$ rather than as either a phase space coordinate or a parameter.

This 6D phase space makes variational analysis straightforward[6]: because coordinate time t is both a good global clock *and* the time parameter for (16), the equations dictating the evolution in t of small separations between trajectories at equal t can be derived just by linearizing Eqs. (18). We perform that linearization now.

C. The variational equations

We work exclusively in the 6D phase space and introduce the following notational simplification. Because the distinction between q's and p's as components of vectors and one-forms, respectively, has to do with their behavior in the 4D manifold of the Kerr spacetime and not with their function in the phase space, where they are merely coordinates labeling points, we will henceforth drop the superscript/subscript distinction. Instead, we will refer to both q^i and p_i as components X_i (with a subscript) of a single six-dimensional coordinate vector

$$\mathbf{X} \equiv \begin{pmatrix} r \\ p_r \\ \theta \\ p_\theta \\ \varphi \\ p_\varphi \end{pmatrix}. \quad (19)$$

This allows us to write Hamilton's equations in the compact form

$$\frac{d\mathbf{X}}{dt} = \mathbf{f}(\mathbf{X}), \quad (20)$$

where the components of $\mathbf{f}$ can be read off Eq. (18).

Now consider an arbitrary reference trajectory $\mathbf{X}(t)$ in phase space and the vector $\delta\mathbf{X}(t)$ of small displacements from points on $\mathbf{X}(t)$ to points at the same coordinate time on neighboring phase trajectories. The first-order equations of motion for $\delta\mathbf{X}(t)$ are the linearized full equations of motion (20) around $\mathbf{X}(t)$. Specifically,

$$\frac{d\delta\mathbf{X}(t)}{dt} = \left.\frac{\partial \mathbf{f}}{\partial \mathbf{X}}\right|_{\mathbf{X}(t)} \delta\mathbf{X}(t) \equiv \mathbf{K}(\mathbf{X}(t))\delta\mathbf{X}(t), \quad (21)$$

or, componentwise,

$$\frac{d\delta X_i(t)}{dt} = K_{ij}(\mathbf{X}(t))\delta X_j(t) \quad (22)$$

$$K_{ij}(\mathbf{X}) \equiv \left.\frac{\partial f_i}{\partial X_j}\right|_{\mathbf{X}} = \left.\frac{\partial f_i}{\partial X_j}\right|_{\text{fixed}_E} + \frac{\partial E}{\partial X_j}\frac{\partial f_i}{\partial E}, \quad (23)$$

where the last equality stems from the caveat regarding Eqs. (18).

Equation (21) is a system of first-order linear ordinary differential equations whose coefficients $K_{ij}(t)$ depend implicitly on time through the solutions $\mathbf{X}(t)$ to (20). The solution to such a system can always be expressed in terms of a fundamental matrix [26] $\mathbf{L}(t; \mathbf{X}_0)$ that depends on the point $\mathbf{X}_0$ on the reference trajectory at which we define the initial displacement vector $\delta\mathbf{X}_0$ and that satisfies

$$\delta\mathbf{X}(t) = \mathbf{L}(t; \mathbf{X}_0)\delta\mathbf{X}_0, \quad (24)$$

where $\mathbf{L}(t = 0; \mathbf{X}_0)$ is the identity matrix.

The goal of variational analysis is to find $\mathbf{L}$, which we can equivalently think of as the time evolution operator for small displacements. Given the equations of motion (20), we can always calculate the matrix $\mathbf{K}$, but in general there is no corresponding analytic expression for $\mathbf{L}$. However, $\mathbf{K}$ on equatorial circular orbits is the constant matrix[7]

$$\mathbf{K} = \frac{1}{\gamma\Sigma} \begin{pmatrix} 0 & \Delta & 0 & 0 & 0 & 0 \\ \frac{R''}{2\Delta} & 0 & 0 & 0 & 0 & \pm\frac{2r^{3/2}}{\gamma\Delta} \\ 0 & 0 & 0 & 1 & 0 & 0 \\ 0 & 0 & \frac{\Theta^{\theta\theta}}{2} & 0 & 0 & 0 \\ \mp\frac{2r^{3/2}}{\gamma\Delta} & 0 & 0 & 0 & 0 & \frac{r^2}{\gamma^2\Delta} \\ 0 & 0 & 0 & 0 & 0 & 0 \end{pmatrix}, \quad (25)$$

where R'' and $\Theta^{\theta\theta}$ are the second derivatives with respect

[6]Using (13) as the Hamiltonian but restricting attention just to the 6D subspace spanned by the spatial coordinates and momenta and tracking $t(\tau)$ as a separate function (as, for instance, in Ref. [23]) would not have been helpful to us. Trajectories would have been bounded in that subspace, but the evolution parameter would still not have been a sensible global clock, and we would have had to synchronize trajectories "by hand." Ultimately, the trade-off of our 6D formulation is "automatic" synchronization of trajectories (since t is a good global clock) at the cost of slightly greater complexity in the equations of motion (18) vs (15). For variational analysis, the formal benefit of the former outweighs the minor drawback of the latter.

[7]Although Eq. (25) can be expressed solely in terms of the black hole spin a and the constant radial coordinate r of the circular orbit, we have left it in this form for readability.

to their arguments of $R(r)$ and $\Theta(\theta)$, respectively, and γ is a shorthand for

$$\gamma \equiv \dot{t}(r)|_{r=\text{circular orbit}}. \tag{26}$$

Since $\mathbf{K}$ is constant, $\mathbf{L}$ has the form[8]

$$\mathbf{L}(t) = e^{\mathbf{K}t} \tag{27}$$

and shares its eigenvectors with $\mathbf{K}$. Finding the eigensolutions of (21) is therefore tantamount to finding eigenvalues and eigenvectors of $\mathbf{K}$.

D. Eigensolutions of the variational equations

The eigenvalues λ of $\mathbf{K}$ are solutions to

$$|\mathbf{K} - \lambda \mathbf{I}| = 0 \tag{28}$$

and come in 3 pairs of equal and opposite eigenvalues whose magnitude we denote as

$$\lambda_r = \frac{1}{\gamma\Sigma}\sqrt{\frac{R''}{2}}, \qquad \lambda_\theta = \frac{1}{\gamma\Sigma}\sqrt{\frac{\Theta^{\theta\theta}}{2}}, \qquad \lambda_\varphi = 0. \tag{29}$$

(See also [2].) The eigensolutions associated with the λ_θ and $\lambda_\varphi = 0$ eigenvalues are extremely revealing in their own right. Presently, however, our concern is the eigensolutions associated with λ_r.

The λ_r may be real or imaginary depending on the sign of

$$\frac{R''}{2} = 12r[1-(1-E^2)r] - 2[a^2(1-E^2) + L_z^2] = -\frac{r^{1/2}(r^2 - 6r \pm 8ar^{1/2} - 3a^2)}{r^{3/2} - 3r^{1/2} \pm 2a}, \tag{30}$$

where we have used the (E, L_z) for circular orbits found in Ref. [27],

$$E = \frac{r^{3/2} - 2r^{1/2} \pm a}{r^{3/4}\sqrt{r^{3/2} - 3r^{1/2} \pm 2a}} \tag{31a}$$

$$L_z = \pm \frac{r^2 \mp 2ar^{1/2} + a^2}{r^{3/4}\sqrt{r^{3/2} - 3r^{1/2} \pm 2a}} \tag{31b}$$

to write R'' in terms of r alone. The plus/minus signs indicate prograde/retrograde. On the unstable circular orbits of interest to us ($r_{\text{ibco}} < r < r_{\text{isco}}$), R'' is positive and λ_r is real and plotted as a function of r for various values of a in Fig. 1.

[8]Considerable analytic insight into $\mathbf{L}$ is also possible when the $\mathbf{K}(t)$ is *periodic* in time t, a situation that arises when the reference trajectory $\mathbf{X}(t)$ is itself periodic and which we tackle for Kerr orbits in a future work.

The (unnormalized) eigenvectors

$$\mathbf{u}_r^{(u)} = \left(\Delta, \sqrt{\frac{R''}{2}}, 0, 0, \mp\frac{2r^{3/2}}{\gamma\sqrt{R''/2}}, 0\right)^T \tag{32}$$

$$\mathbf{u}_r^{(s)} = \left(\Delta, -\sqrt{\frac{R''}{2}}, 0, 0, \pm\frac{2r^{3/2}}{\gamma\sqrt{R''/2}}, 0\right)^T \tag{33}$$

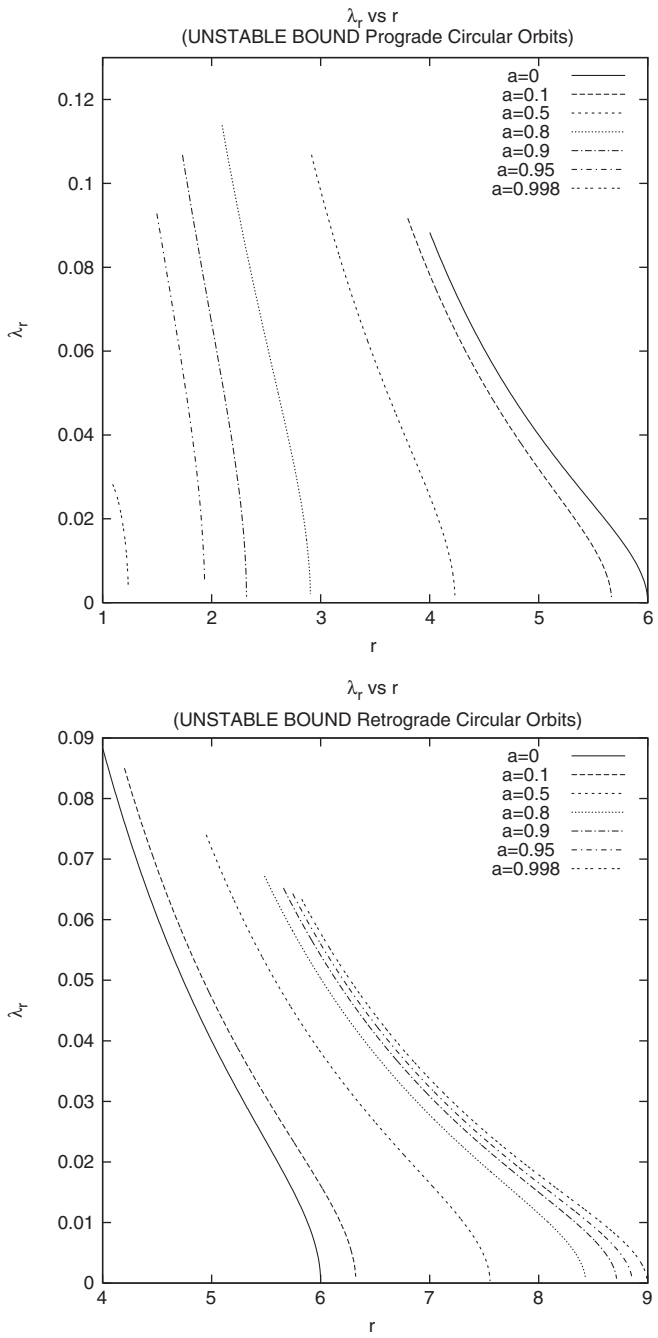

FIG. 1. The dimensionless real-valued stability exponent λ_r (measured in units of M^{-1}) for unstable circular orbits with $E < 1$ for various spins a. Left: Prograde orbits. Right: Retrograde orbits.

associated with $\pm\lambda_r$ are also real. Combining (24) and (27), each eigenvalue/eigenvector pair yields a corresponding eigensolution

$$\delta\mathbf{X}_\mathbf{r}^{(\mathbf{u})}(t) = c^{(u)}e^{+\lambda_r t}\mathbf{u}_r^{(u)} \qquad \delta\mathbf{X}_\mathbf{r}^{(\mathbf{s})}(t) = c^{(s)}e^{-\lambda_r t}\mathbf{u}_r^{(s)} \tag{34}$$

to the variational equation (21), where the constants $c^{(u,s)}$ reflect where we choose to set $t = 0$.

E. Relation to the homoclinic orbits

We now build the case that in the neighborhood of $\mathbf{X}^{\rm circ}(t)$, the linearized solutions $\mathbf{X}^{(\mathbf{u},\mathbf{s})}(t)$ coincide with exact homoclinic solutions $\mathbf{X}^{\rm hc}(t)$. For simplicity, we focus on the unstable solution in (34), which corresponds to a linearized solution

$$\mathbf{X}^{(\mathbf{u})}(t) = \mathbf{X}^{\rm circ}(t) + \delta\mathbf{X}_\mathbf{r}^{(\mathbf{u})}(t) \tag{35}$$

to the full equations of motion (20) [the results are analogous for $\mathbf{X}^{(\mathbf{s})}(t)$].

Some of the similarities between the linearized and homoclinic orbit are self-evident. The absence of θ and p_θ components in $\mathbf{X}^{(\mathbf{u})}(t)$ indicates that the orbit remains equatorial, and the identical signs on the r and p_r components reflect the fact that small displacements from the circular orbit along the eigendirection run away exponentially to larger radial positions and velocities on an e-folding time scale λ_r^{-1}. The absence of a p_φ component in $\delta\mathbf{X}_\mathbf{r}^{(\mathbf{u})}(t)$ indicates that the linearized orbit has the same angular momentum L_z as $\mathbf{X}^{\rm circ}(t)$.

Less self-evident is the fact that, like the homoclinic orbit, the linearized orbit also has the same energy E as the circular orbit. To see this, note that since the Hamiltonian $E = E(\mathbf{X})$ is a function of the phase space coordinates, the energy difference $\delta E = E^{\rm circ} - E^{\rm lin}$ can be expanded as a power series in the components of $\delta\mathbf{X}_\mathbf{r}^{(\mathbf{u})}$. Because the derivatives of all phase variables except φ vanish on the circular orbit and $\delta p_\varphi = 0$, the first-order contribution to that expansion vanishes,

$$\begin{aligned}\delta E^{(1)} &= \frac{\partial H_{6D}}{\partial x^i}\bigg|_{r_u}\delta x^i + \frac{\partial H_{6D}}{\partial p_i}\bigg|_{r_u}\delta p_i \\ &= -\frac{dp_i}{dt}\bigg|_{r_u}\delta x^i + \frac{dx^i}{dt}\bigg|_{r_u}\delta p_i = \frac{d\varphi}{dt}\delta p_\varphi = 0.\end{aligned} \tag{36}$$

The second order variation in the energy becomes

$$\begin{aligned}\delta E^{(2)} &= \frac{\partial^2 H_{6D}}{\partial x^i\partial x^j}\bigg|_{r_u}\delta x^i\delta x^j + \frac{\partial^2 H_{6D}}{\partial p_i\partial p_j}\bigg|_{r_u}\delta p_i\delta p_j \\ &\quad + 2\frac{\partial^2 H_{6D}}{\partial x^i\partial p_j}\bigg|_{r_u}\delta x^i\delta p_j \\ &= -\frac{\partial}{\partial x^i}\frac{dp_j}{dt}\bigg|_{r_u}\delta x^i\delta x^j + \frac{\partial}{\partial p_i}\frac{dx^j}{dt}\bigg|_{r_u}\delta p_i\delta p_j \\ &\quad + 2\frac{\partial}{\partial x^i}\frac{dx^j}{dt}\bigg|_{r_u}\delta x^i\delta p_j \\ &= -\frac{\partial}{\partial r}\frac{dp_r}{dt}\bigg|_{r_u}\delta r^2 + \frac{\partial}{\partial p_r}\frac{dr}{dt}\bigg|_{r_u}\delta p_r^2 \\ &\quad + 2\frac{\partial}{\partial r}\frac{dr}{dt}\bigg|_{r_u}\delta r\delta p_r \\ &= -K_{p_r r}|_{r_u}\delta r^2 + K_{rp_r}|_{r_u}\delta p_r^2 + 2K_{rr}|_{r_u}\delta r\delta p_r.\end{aligned} \tag{37}$$

Using Eq. (25) and the fact that

$$\delta p_r = \frac{1}{\Delta}\sqrt{\frac{R''}{2}}\delta r \tag{38}$$

on the eigensolution, we find that

$$\begin{aligned}\delta E^{(2)} &= \frac{\delta r^2}{\gamma\Sigma}\left(-K_{p_r r}|_{r_u} + K_{rp_r}|_{r_u}\frac{R''}{2\Delta^2} + 2K_{rr}|_{r_u}\sqrt{\frac{R''}{2\Delta^2}}\right) \\ &= \frac{\delta r^2}{\gamma\Sigma}\left(\frac{R''}{2\Delta} + \Delta\left(\frac{1}{\Delta^2}\right)\frac{R''}{2} + 0\right) = 0.\end{aligned} \tag{39}$$

A similar result holds for $\mathbf{X}^{(\mathbf{s})}(t)$, despite the addition of an overall minus sign in (38), since through second order δE depends on δp_r^2. Continuing this process to higher orders is beyond the algebraic patience of the authors, but at least through second order in the variations, the linearized solutions describe orbits with the same E and L as the unstable circular orbit.

The φ component of $\delta\mathbf{X}_\mathbf{r}^{(\mathbf{u})}(t)$ merits more discussion. The ratio $\delta\varphi/\delta r$ is fixed, so that $\delta\varphi$ does not merely represent an arbitrary overall translation in φ. Instead, this component indicates how the phasing difference between the linearized orbit and the circular orbit changes as the radial separation between the two orbits grows. Notice also that since $\delta\mathbf{X}_\mathbf{r}^{(\mathbf{u})}(t) \to 0$ as $t \to -\infty$ regardless of how $c^{(u)}$ is chosen, the linearized solution describes an orbit that is in phase with the circular orbit in the infinite past. There is a unique choice of phase for a homoclinic orbit that will synchronize it with the circular orbit in the infinite past [18]. Apparently, the linearized eigensolution goes so far as to select the *phase* of the homoclinic orbit it locally approximates.[9] The import is that the linearization captures

[9]Of course we can have a homoclinic orbit of any phase still line up with the linearized solution simply by adding an overall φ shift to $\delta\mathbf{X}_\mathbf{r}^{(\mathbf{u})}(t)$.

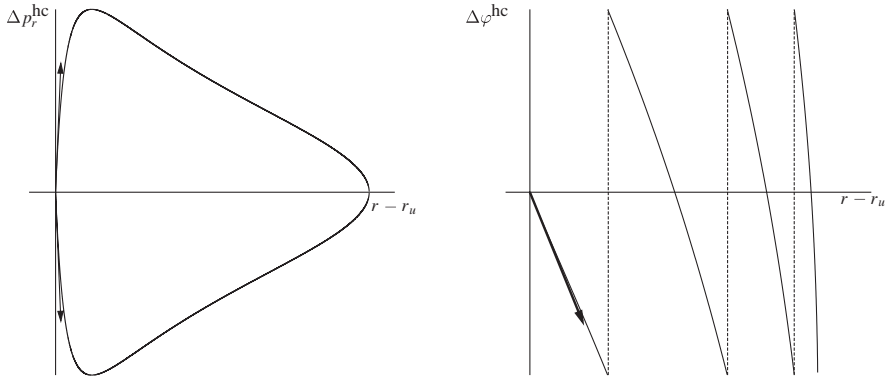

FIG. 2. Projections of the eigenvector $\mathbf{u}_r^{(u)}$, to which the linearized separation $\delta\mathbf{X}^{(u)}$ is proportional, overlayed with the actual coordinate differences $\mathbf{X}^{\rm hc} - \mathbf{X}^{\rm circ}$ in the phase space. In the $\Delta\varphi$ plot, we have identified $-\pi$ at the bottom of the plot and π at the top. The plots, intended to be schematic, are around an unstable circular orbit at $r_u = 2.2$ for $a = 0.8$.

detailed information about neighboring orbits, including phase information.

Analogously, the linearized solution

$$\mathbf{X}^{(\mathbf{s})}(t) = \mathbf{X}^{\rm circ}(t) + \delta\mathbf{X}_{\mathbf{r}}^{(\mathbf{s})}(t) \tag{40}$$

synchronizes with the circular orbit at $t = +\infty$. We can now understand the signs of the $\delta\varphi$ components of both eigenvectors. In $\delta\mathbf{X}_{\mathbf{r}}^{(\mathbf{u})}(t)$ it has the opposite sign as δr because as the displaced orbit moves to larger r, its $d\varphi/dt$ drops, and it *lags* the circular orbit with which it was synchronized at $t = -\infty$. In $\delta\mathbf{X}_{\mathbf{r}}^{(\mathbf{s})}(t)$, in contrast, $\delta\varphi$ and δr have the same sign: since the circular orbit will accumulate azimuth faster than the displaced orbit as it spirals in, it must begin *ahead* of the circular orbit in phase if the two are to synchronize at $t = +\infty$.

Now, the two linearized solutions $\mathbf{X}^{(\mathbf{u})}(t)$ and $\mathbf{X}^{(\mathbf{s})}(t)$ do not coincide with the same homoclinic orbit, but rather with two homoclinic orbits that differ by a phase. Since circular orbits that differ by a phase belong to the same invariant set, we continue to refer to these as homoclinic and not heteroclinic trajectories.

F. Phase portraits

To make the coincidence between the linearized solutions and the homoclinic orbits manifest, we examine a phase portrait of the homoclinic orbit and the linearized solutions. Again, we use the radial coordinate r along the homoclinic orbit as our global time parameter. The required expression for p_r in terms of r for the homoclinic orbit follows from Eq. (15a). The result is

$$p_r(r) = \frac{\sqrt{R(r)}}{\Delta} \tag{41}$$

for outbound motion and the negative of the same expression for inbound motion. Together with the exact solutions from paper I [18], (41) generates the exact phase curves of the homoclinic orbit. Figure 2 overlays a homoclinic orbit and the corresponding linearized orbit $\mathbf{X}^{(\mathbf{u})}$. By construction, the orbits are coincident at $t = -\infty$.

For illustration, we have plotted the case $a = 0.8$ with an associated unstable circular orbit at $r_u = 2.500\,536$. Since both orbits are equatorial (so that θ motion can be suppressed) and have the same L_z, a 3D orbit in r, p_r, φ space captures all the dynamical information, and each panel of Fig. 2 shows the projections of the two orbits into a plane. The curves in Fig. 2 are the coordinate separations between the homoclinic and circular orbits, with the various projections of the separation eigenvectors overlayed. They confirm that the global stable and unstable manifolds of the circular orbits are tangent at the circular orbits to the local stable and unstable manifolds defined by the eigensolutions to the variational equations.

G. Action-angle variables

In an action-angle formulation [23,25,28] of Kerr motion, the Hamiltonian is reformulated in terms of constant momenta J_i called actions and canonically conjugate angle variables ψ_i that increase linearly with time at rates ω_i. Fourier expansions of orbit functionals in terms of the fundamental frequencies ω_i are the basis of frequency-domain radiative evolution codes, and Ref. [24] develops a description of the inspiral dynamics entirely in terms of action-angle variables. For completeness, we include exact expressions for the frequencies and actions of homoclinic orbits.

1. Fundamental frequencies

Because the equatorial Kerr system is two dimensional and integrable, every bound orbit has an associated pair of fundamental frequencies[10]

[10]Even equatorial orbits have a third frequency ω_θ associated with small oscillations about the equatorial plane. We discuss the significance of these frequencies for all equatorial orbits in a separate work.

$$\omega_r \equiv \frac{2\pi}{T_r} \tag{42a}$$

$$\omega_\varphi \equiv \frac{1}{T_r}\int_0^{T_r}\left|\frac{d\varphi}{dt}\right| dt = \frac{\int_{r_p}^{r_a} dr|\frac{d\varphi}{dr}|}{\int_{r_p}^{r_a} dr\frac{dt}{dr}}. \tag{42b}$$

Because their radial period is infinite, $\omega_r = 0$ for homoclinic orbits. Homoclinic orbits also whirl an infinite amount as they approach their periastron r_u, so both the numerator and denominator of (42b) diverge.

However, the divergences in both T_r and the accumulated azimuth φ can be traced to specific terms of the form [18]

$$\begin{aligned}\varphi &\to 2\frac{\Omega_u}{\lambda_r}\tanh^{-1}\sqrt{\frac{r_u}{r}\frac{r_a-r}{r_a-r_u}},\\ t &\to 2\frac{1}{\lambda_r}\tanh^{-1}\sqrt{\frac{r_u}{r}\frac{r_a-r}{r_a-r_u}} \quad \text{as } t\to T_r=\infty,\\ r &\to r_u.\end{aligned} \tag{43}$$

Their ratio thus converges to $\Omega_u \equiv d\varphi/dt(r_u)$, the constant coordinate velocity of the circular orbit at r_u.

The azimuthal frequency for the homoclinic orbit and its associated unstable circular orbit are thus the same,

$$\omega_r^{\rm hc} = 0, \qquad \omega_\varphi^{\rm hc} = |\Omega_u| = \frac{1}{r_u^{3/2}+a^2}. \tag{44}$$

That allows us to make a nice statement: the stable and unstable circular orbits determine the lower and upper bounds, respectively, of the ω_φ's of all eccentric bound orbits with a given $|L_{\rm isco}| < |L_z| < |L_{\rm ibco}|$.

2. Actions

Each action J_i of a bound orbit is defined by

$$J_i \equiv \oint p_i dq_i, \tag{45}$$

where the integral is taken over the projection of the orbit into the q_i, p_i plane. Since $p_\varphi = L_z$ is constant, $J_\varphi = 2\pi L_z$ for any orbit. The radial action J_r is the area enclosed by closed (r, p_r) curves like that of Fig. 2,

$$J_r \equiv \oint p_r(r)dr = 2\int_{r_p}^{r_a} dr\frac{\sqrt{R(r)}}{\Delta}. \tag{46}$$

For arbitrary orbits, (46) at best reduces to elliptic integrals, but for the homoclinic orbit, J_r can be written as an exact function of r_u alone. The result, derived in the Appendix, is

$$\begin{aligned}J_r^{\rm hc} = 2\sqrt{1-E^2}\times\Bigg\{&-\sqrt{r_u(r_a-r_u)}\\ &+2\frac{2E^2-1}{1-E^2}\tan^{-1}\sqrt{\frac{r_a-r_u}{r_u}}\Bigg\}+\frac{2}{\sqrt{1-a^2}}\\ &\times\Bigg\{\sqrt{R(r_-)}\tanh^{-1}\sqrt{\frac{r_-}{r_a-r_-}\frac{r_a-r_u}{r_u}}\\ &-\sqrt{R(r_+)}\tanh^{-1}\sqrt{\frac{r_+}{r_a-r_+}\frac{r_a-r_u}{r_u}}\Bigg\}.\end{aligned} \tag{47}$$

III. CONCLUSION

Although the results of this paper are self-contained, the phase space portrait is a direct complement to the physical space portrait of paper I [18]. Both approaches identify the separatrix between bound and plunging orbits with a homoclinic trajectory that whirls an infinite number of times on asymptotic approach to a circle.

The Hamiltonian variational analysis detailed in this paper yields descriptions of group flows of orbits. Although the intention was to detail a profile of the separatrix, the technical results of this paper could have further utility. In particular, the whirling stages of trajectories in the vicinity of the homoclinic set might be modeled as variations around the circular orbit using the eigenvectors and eigenvalues found here. In the future, we aim to generalize this approach to capture orbits around the periodic set [21] and to move out of the equatorial plane [29,30].

Another connection that should be made in a dynamical discussion of the separatrix is its role as the divide between chaotic and nonchaotic behavior. The geodesic motion of a nonspinning test particle around a Kerr black hole is known to be integrable [22]. There are as many constants of motion as there are canoncial momenta in this Hamiltonian system.

However, the presence of a homoclinic orbit indicates the Kerr system is at least vulnerable to chaos [31–34]. Under perturbation, the stable and unstable manifolds that previously coincided along the homoclinic orbit (Fig. 2) could develop transverse intersections. In other words, the stable and unstable manifolds would not coincide but rather intersect, and once they intersected, would do so an infinite number of times creating a homoclinic tangle, as in Fig. 3. The homoclinic tangle is associated with a fractal set of periodic orbits and, when it appears, marks a locus of chaotic behavior in dynamical systems.

Chaotic behavior has in fact already been found for test particle motion in a Schwarzschild background perturbed by gravitational waves from a third body [31], for spinning test particle motion around Schwarzschild [32,33] and Kerr [35] black holes (albeit only for unphysically large values of test particle spin) and in the case of spinning comparable mass black holes [35–41], for which homoclinic orbits at

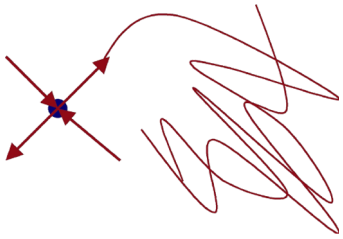

FIG. 3 (color online). Schematic of a homoclinic tangle. The curve above represents the repeated intersection of a homoclinic orbit of the perturbed system with the r, p_r phase plane. The large dot represents the intersection of a circular orbit in the perturbed system along with the eigenvectors denoting its local stable and unstable manifolds.

third post-Newtonian order in the absence of radiation have also been shown to exist [30].

While this paper is concerned with Kerr orbits, we mention in closing that the chaotic orbits of comparable mass binaries—in the absence of radiation reaction—could be evidence of a homoclinic tangle [30]. Chaos in the PN approximation of comparable mass pairs of spinning black holes was found in Refs. [36,37] and has since been confirmed[11] by several independent groups [35,38,41]. Yet for comparable mass pairs, losses due to gravitational radiation could happen on a shorter time scale and effectively quash the chaotic behavior [20,35,38], like a pinball game with too much friction. However, due to the challenges the strong-field regime poses for the post-Newtonian approximation methods, the competition between time scales is not easily resolved [19,20,39]. Numerical solutions to the fully nonlinear Einstein equations have shown no evidence of chaotic behavior to date. Still, the computational expense of such simulations means only a tiny fraction of the parameter space has been explored. There remains no definitive answer to the question of whether or not chaos will ever be observed in astrophysical black hole pairs. Chaotic orbits, if they are ever observed, could be evidence of a homoclinic tangle in the most nonlinear regimes of black hole spacetimes.

[11]Although our concern is with Kerr orbits, we digress for a moment to address an issue raised in review. Reference [42] noted that under the restricted circumstance of only one body spinning and/or equal mass binaries, there should not be chaos in a PN Hamiltonian description of two black holes with only spin-orbit coupling included: under these restrictions, there are enough constants of motion to ensure regular behavior. However, [36] found chaos even when only one body was spinning, in seeming contradiction with [42]. The inconsistency is only apparent. The presence or absence of chaos is a property of the specific equations of motion, and the detection of chaos in the Lagrangian formulation of [36] is not inconsistent with the claimed absence chaos in the Hamiltonian formulation of [42]. Indeed, it is expected that small perturbations to the Hamiltonian system would display chaos, and the Lagrangian formulation can be viewed as a small perturbation to the Hamiltonian system (at higher order than the validity of the approximation). This issue was resolved in [43] and followed up in [40,41].

ACKNOWLEDGMENTS

We are especially grateful to Becky Grossman for her valuable and generous contributions to this work. We also thank Bob Devaney for helpful input concerning dynamical systems language. J. L. and G. P.-G. acknowledge financial support from a Columbia University ISE grant. This material is based upon work supported under a National Science Foundation Graduate Research Fellowship.

APPENDIX: DERIVATION OF ACTION OF HOMOCLINIC ORBITS

The radial action of a bound nonplunging orbit is the area enclosed by its projection into the r, p_r plane,

$$J_r \equiv \oint p_r(r)dr = 2\int_{r_p}^{r_a} dr \frac{\sqrt{R(r)}}{\Delta}, \tag{A1}$$

where r_p and r_a are the periastron and apastron, respectively, and $R(r)$ is the function (5).

For a homoclinic orbit, r_p equals r_u, the radius of the associated unstable circular orbit, and r_a is expressible in terms of r_u alone [18]. Additionally, $R(r)$ factors into

$$R(r) = (1 - E^2)r(r - r_u)^2(r_a - r), \tag{A2}$$

with E the common energy of the homoclinic and unstable circular orbit. The orbit independent quantity Δ can always be factored into

$$\Delta = (r - r_+)(r - r_-), \tag{A3}$$

where $r_\pm \equiv 1 \pm \sqrt{1 - a^2}$ are the outer and inner horizons, respectively, of the central black hole. Together, the above allows us to write the radial action (A1) of a homoclinic orbit as

$$\begin{aligned}\frac{J_r^{\rm hc}}{2\sqrt{1 - E^2}} &= \int_{r_u}^{r_a} dr \frac{(r - r_u)\sqrt{r(r_a - r)}}{(r - r_+)(r - r_-)} \\ &= \int_{r_u}^{r_a} dr \sqrt{\frac{r_a - r}{r}} \frac{r(r - r_u)}{(r - r_+)(r - r_-)}.\end{aligned} \tag{A4}$$

The integral in (A4) can be done analytically. Under the change of variable

$$\begin{aligned} u &= \sqrt{\frac{r}{r_a - r}}, \qquad r = \frac{u^2}{u^2 + 1} r_a \\ dr\sqrt{\frac{r_a - r}{r}} &= du \frac{2r_a}{(1 + u^2)^2}, \end{aligned} \tag{A5}$$

the factors in (A4) become

$$\begin{aligned} r_a - r &= \frac{r_a}{1+u^2}, \\ r - r_u &= \frac{u^2(r_a - r_u) - r_u}{1+u^2}, \\ r - r_+ &= \frac{u^2(r_a - r_+) - r_+}{1+u^2}, \\ r - r_- &= \frac{u^2(r_a - r_-) - r_-}{1+u^2} \end{aligned} \tag{A6}$$

and (A4) becomes

$$\frac{J_r^{\rm hc}}{2\sqrt{1-E^2}} = \frac{r_a - r_u}{(r_a - r_+)(r_a - r_-)} \times \int_{u_u}^{\infty} du \frac{2r_a^2 u^2[u^2 - u_u^2]}{(1+u^2)^2[u^2 - u_+^2][u^2 - u_-^2]}, \tag{A7}$$

where

$$u_u^2 \equiv \frac{r_u}{r_a - r_u}, \qquad u_+^2 \equiv \frac{r_+}{r_a - r_+}, \qquad u_-^2 \equiv \frac{r_-}{r_a - r_-}. \tag{A8}$$

The integral in (A7) decomposes by partial fractions into

$$\frac{J_r^{\rm hc}}{2\sqrt{1-E^2}} = (A_1 \mathcal{I}_1 + A_2 \mathcal{I}_2 + A_3 \mathcal{I}_3 + A_4 \mathcal{I}_4)|_{u_u}^{\infty}, \tag{A9}$$

where the coefficients A_i are

$$A_1 = r_a, \qquad A_2 = 2(r_u - 2), \qquad A_3 = \frac{r_-(r_u - r_-)}{\sqrt{1-a^2}}, \qquad A_4 = -\frac{r_+(r_u - r_+)}{\sqrt{1-a^2}}. \tag{A10}$$

and the functions $\mathcal{I}_i$ are

$$\mathcal{I}_1 \equiv \int du \frac{2}{(1+u^2)^2} = \frac{u}{1+u^2} + \tan^{-1} u, \tag{A11a}$$

$$\mathcal{I}_2 \equiv \int du \frac{1}{1+u^2} = \tan^{-1} u, \tag{A11b}$$

$$\mathcal{I}_3 \equiv \int du \frac{1}{u^2 - u_-^2} = \frac{1}{2}\sqrt{\frac{r_a - r_-}{r_-}} \ln\left[\frac{u - u_-}{u + u_-}\right], \tag{A11c}$$

$$\mathcal{I}_4 \equiv \int du \frac{1}{u^2 - u_+^2} = \frac{1}{2}\sqrt{\frac{r_a - r_+}{r_+}} \ln\left[\frac{u - u_+}{u + u_+}\right]. \tag{A11d}$$

The right-hand side of (A9) is easiest to evaluate in pieces. The first two terms give

$$\begin{aligned} (A_1 \mathcal{I}_1 + A_2 \mathcal{I}_2)|_{u_u}^{\infty} &= -r_a \frac{u_u}{1+u_u^2}(r_a + 2r_u - 4)\left(\frac{\pi}{2} - \tan^{-1} u_u\right) = -\sqrt{r_u(r_a - r_u)} + (r_a + 2r_u - 4)\left(\tan^{-1}\frac{1}{u_u}\right) \\ &= -\sqrt{r_u(r_a - r_u)} + 2\frac{2E^2 - 1}{1 - E^2}\tan^{-1}\sqrt{\frac{r_a - r_u}{r_u}}. \end{aligned} \tag{A12}$$

To go from the first to the second line in (A12), we have used $\tan^{-1}(u) + \tan^{-1}(1/u) = \pi/2$. To get the last line, we have used the fact that

$$r_a + 2r_u = \frac{2}{1 - E^2} \tag{A13}$$

for homoclinic orbits, which follows from equating the cubic coefficients in Eqs. (5) and (A2).

The third term in (A9) is

$$\begin{aligned} A_3 \mathcal{I}_3|_{u_u}^{\infty} &= -\frac{1}{2}\frac{(r_u - r_-)\sqrt{r_-(r_a - r_-)}}{\sqrt{1-a^2}} \ln\left[\frac{u_u - u_-}{u_u + u_-}\right] = \frac{1}{2}\frac{1}{\sqrt{1-a^2}}\sqrt{\frac{R(r_-)}{1-E^2}} \ln\left[\frac{u_u + u_-}{u_u - u_-}\right] \\ &= \frac{1}{\sqrt{1-a^2}}\sqrt{\frac{R(r_-)}{1-E^2}}\tanh^{-1}\frac{u_-}{u_u} = \frac{1}{\sqrt{1-a^2}}\sqrt{\frac{R(r_-)}{1-E^2}}\tanh^{-1}\sqrt{\frac{r_-}{r_a - r_-}\frac{r_a - r_u}{r_u}}, \end{aligned} \tag{A14}$$

and likewise

$$A_4 \mathcal{I}_4|_{u_u}^{\infty} = -\frac{1}{\sqrt{1-a^2}}\sqrt{\frac{R(r_+)}{1-E^2}}\tanh^{-1}\sqrt{\frac{r_+}{r_a - r_+}\frac{r_a - r_u}{r_u}}. \tag{A15}$$

Combining (A9), (A12), (A14), and (A15), we find that

$$J_r^{\rm hc} = 2\sqrt{1-E^2}\times\left\{-\sqrt{r_u(r_a-r_u)}+2\frac{2E^2-1}{1-E^2}\tan^{-1}\sqrt{\frac{r_a-r_u}{r_u}}\right\}$$
$$+\frac{2}{\sqrt{1-a^2}}\left\{\sqrt{R(r_-)}\tanh^{-1}\sqrt{\frac{r_-}{r_a-r_-}\frac{r_a-r_u}{r_u}}-\sqrt{R(r_+)}\tanh^{-1}\sqrt{\frac{r_+}{r_a-r_+}\frac{r_a-r_u}{r_u}}\right\}. \quad \text{(A16)}$$

[1] L. Barack and A. Ori, Phys. Rev. Lett. **90**, 111101 (2003).
[2] F. Pretorius, Classical Quantum Gravity **23**, S529 (2006).
[3] F. Herrmann, I. Hinder, D. Shoemaker, P. Laguna, and R. A. Matzner, Astrophys. J. **661**, 430 (2007).
[4] M. Campanelli, C. O. Lousto, Y. Zlochower, B. Krishnan, and D. Merritt, Phys. Rev. D **75**, 064030 (2007).
[5] M. Campanelli, C. O. Lousto, P. Marronetti, and Y. Zlochower, Phys. Rev. Lett. **96**, 111101 (2006).
[6] J. G. Baker, J. Centrella, D.-I. Choi, M. Koppitz, and J. van Meter, Phys. Rev. Lett. **96**, 111102 (2006).
[7] P. Marronetti *et al.*, Classical Quantum Gravity **24**, S43 (2007).
[8] M. A. Scheel *et al.*, Phys. Rev. D **74**, 104006 (2006).
[9] Z. B. Etienne, J. A. Faber, Y. T. Liu, S. L. Shapiro, and T. W. Baumgarte, Phys. Rev. D **76**, 101503 (2007).
[10] U. Sperhake, Phys. Rev. D **76**, 104015 (2007).
[11] Z. Cao, H.-J. Yo, and J.-P. Yu, Phys. Rev. D **78**, 124011 (2008).
[12] E. E. Flanagan and S. A. Hughes, Phys. Rev. D **57**, 4535 (1998).
[13] K. Glampedakis, S. A. Hughes, and D. Kennefick, Phys. Rev. D **66**, 064005 (2002).
[14] S. Drasco and S. A. Hughes, Phys. Rev. D **69**, 044015 (2004).
[15] S. Drasco, E. E. Flanagan, and S. A. Hughes, Classical Quantum Gravity **22**, S801 (2005).
[16] S. Drasco and S. Hughes, Phys. Rev. D **73**, 024027 (2006).
[17] R. N. Lang and S. A. Hughes, Phys. Rev. D **74**, 122001 (2006).
[18] J. Levin and G. Perez-Giz, preceding Article, Phys. Rev. D **79**, 124013 (2009).
[19] N. J. Cornish, Phys. Rev. D **64**, 084011 (2001).
[20] N. J. Cornish and J. Levin, Classical Quantum Gravity **20**, 1649 (2003).
[21] J. Levin and G. Perez-Giz, Phys. Rev. D **77**, 103005 (2008).
[22] B. Carter, Phys. Rev. **174**, 1559 (1968).
[23] W. Schmidt, Classical Quantum Gravity **19**, 2743 (2002).
[24] T. Hinderer and E. E. Flanagan, (unpublished).
[25] A. Lichtenberg and M. Liberman, *Regular and Choatic Dynamics* (Springer, New York, 1992).
[26] W. E. Boyce and R. C. DiPrima, *Elementary Differential Equations and Boundary Value Problems* (Wiley, New York, 2005).
[27] J. M. Bardeen, W. H. Press, and S. A. Teukolsky, Astrophys. J. **178**, 347 (1972).
[28] K. Glampedakis, Classical Quantum Gravity **22**, S605 (2005).
[29] J. Levin and R. Grossman, Phys. Rev. D **79**, 043016 (2009).
[30] R. Grossman and J. Levin, (unpublished).
[31] L. Bombelli and E. Calzetta, Classical Quantum Gravity **9**, 2573 (1992).
[32] S. Suzuki and K.-i. Maeda, Phys. Rev. D **55**, 4848 (1997).
[33] S. Suzuki and K.-i. Maeda, Phys. Rev. D **61**, 024005 (1999).
[34] K. Kiuchi and K.-i. Maeda, Phys. Rev. D **70**, 064036 (2004).
[35] M. D. Hartl, Phys. Rev. D **67**, 024005 (2003).
[36] J. Levin, Phys. Rev. Lett. **84**, 3515 (2000).
[37] J. Levin, Phys. Rev. D **67**, 044013 (2003).
[38] M. D. Hartl and A. Buonanno, Phys. Rev. D **71**, 024027 (2005).
[39] N. J. Cornish and J. J. Levin, Phys. Rev. D **68**, 024004 (2003).
[40] X. Wu and Y. Xie, Phys. Rev. D **76**, 124004 (2007).
[41] X. Wu and Y. Xie, Phys. Rev. D **77**, 103012 (2008).
[42] C. Königsdoerffer and A. Gopakumar, Phys. Rev. D **71**, 024039 (2005).
[43] J. Levin, Phys. Rev. D **74**, 124027 (2006).